Supplementary material

Flow cytometry on Cohort#1(A&B) and DC identification

PBMCs were thawed in 10mL preheated RPMI 1640 Glutamax (Gibco) with 1% penicillin/streptomycin, washed, counted, and 1 million cells were lived/dead stained using 0.1 µL LIVE/DEAD™ Fixable Near-IR Dead Cell Stai n Kit, for 633 or 635 nm excitation (Invitrogen, Thermo Fisher Scientific) in 80 µL DPBS (Biowest), followed by a DPBS wash, and subsequent blocking in 100 µL 10% heat-inactivated (HI) human AB Serum (H4522 Sigma) in DPBS. Cells were stained with anti-human cell surface fluorochrome-conjugated antibodies according to **Supp.Table 3** in a total volume of 100 µL DPBS with 1% Albumin fraction V, from bovine serum (Merck). After additional washing and fixation in 0.9% formaldehyde (SigmaAldrich) in DPBS, the cells were stored at 4^{o}C for 1-3 days and run on a LSR Fortessa flow cytometer (BD) equipped with a 405 nm, 488 nm, 561 nm and 640 nm laser. A compensation matrix was calculated using single stains on OneComp eBeads (Thermo Fischer Scientific) and ArC Armine reactive compensation bead kit (Invitrogen) for antibodies and live/dead stain, respectively. Daily cytometer voltage settings were confirmed using SPHERO^{TM} Rainbow calibration Particles (BD Bioscience) reassuring the same MFI in all open channels for at least three peaks. Beforehand, all antibodies were titrated on at least five different dilutions of single stains. Prober compensation and gating were confirmed on fluorescence minus one (FMO) samples. Patient subgroups and controls were evenly distributed in different experiments, and for each experiment, aliquots from the same control donor were stained to test any day-to-day variation and antibody lot number variation. Antibody lot differences affected TLR4; thus, only the 66 samples where the same TLR4 antibody lot were used are included in the analyses. FSC files were analyzed blinded using FlowJo V10 with the following gating strategy for Cohort#1A&B (**Supp.Fig.3**): Single cells were identified on FSC-A vs. FSC-H followed by SSC-A vs. SSC-H, debris was excluded on a FSC-A vs. SSC-A plot, cytometer stability was gated on time vs. CD163 PE-A, with subsequent exclusion of dead cells on live/dead vs. SSC-A. Monocytes/ dendritic cells (DCs), thus mononuclear phagocytes (MNPs) (TLR2^{+}), the precursor NK cells (CD56^{bright}/TLR2^{-}/CD16^{-}), and mature NK cells (CD56^{dim}/TLR2^{-}/CD16$^{+/-}$) were identified on CD56 ECD-A vs. TLR2 APC-A with CD16 and CD11b heat-mapping as guidance. From the MNP gate, several different populations were identified: CD14 BV421-A vs. CD16

PC7-A with HLA-DR heat-mapping (based on its high monocytic discrimination index (1, 2)) identified monocyte subtypes (classical-, intermediate-, non-classical, and unclassified (DCs) monocytes); CD163 PE-A vs CCR2 FITC-A (fixed gating); CD11b SB780-A vs. CCR2 FITC-A with CD163 heat-mapping (for the CCR2/CD11b double^{+} population, the majority was also CD163^{+}). Frequencies of single maker expression on MNPs and other subpopulations were gated (fixed) against SSC-A. Median fluorescence intensity (MFI) was calculated on gates with only a single peak, or on priory positive/bright-gated cells as indicated.
A plot was conducted on ten concatenated samples of live cells from all patient and control groups to confirm gating strategy and explore co-expression of different receptors.

To examine the DC distribution, we used another antibody panel (**Supp.Table 3**) and gating strategy on three control samples (**Suppl.Fig4**): Similar gating approach as described above was used to reach MNP subtyping (Q1-4), except no gate on time. From the live cell gate, conventional DC type 1 (cDC1) and plasmacytoid (p)DCs were identified on dot plot with TLR2 APC-A vs. CD141 BV510-A or CD303 PerCP-eFlour710-A, respectively (2). With a fraction of B cells also being CD1c positive, the cDC type 2 (cDC2) was identified from the MNP gate on a CD1c PE-A vs. SSC dot plot. cDC2 was back-gated on MNP subtypes (Q1-4) and to the MNP main gate together with cDC1 and pDC back-gating. From the Q4 gate on the CD14 BV421-A vs. CD16 PC7-A MNP subtyping dot plot, CD1c PE-A vs. CD11c FITC-A was used to define the actual DCs within this gate.

Supplementary Table 1: Clinical details for the longitudinal Cohort#1B

ID+visit	Days from V1	Month from V1	Age at onset	Age at visit	Disease duration	LEDD	H&Y	UPDRS III	MoCA	MMSE
EPM21.v1	-	-	66	68	2	100	1	7	29	29
EPM21.v2	192	6	66	69	3	100	1	10	29	30
EPM21.v3	366	12	66	69	3	-	1	10	28	29
EPM23.v1	-	-	73	77	4	-	2	30	24	26
EPM23.v2(L)	328	11	73	78	5	643	2	41	27	29
LPM21.v1	-	-	65	72	7	965	3	21	29	27
LPM21.v2	184	6	65	73	8	1213	3	28	25	30
LPM21.v3	359	12	65	73	8	1213	2	11	26	27
LPM21.v4	506	16.7	65	73	8	1307	2	23	28	28
LPM22.v1	-	-	58	67	9	920	2	37	28	30
LPM22.v2	181	6	58	68	10	900	3	25	28	30
LPM22.v3	355	12	58	68	10	900	2	19	30	29
LPM23.v1	-	-	47	62	15	1454	2	29	28	29
LPM23.v2	35	1	47	62	15	1087	2	42	30	29
LPM24.v1	-	-	51	56	5	420	3	70	26	29
LPM24.v2	159	5	51	57	6	500	2	59	28	29
LPM24.v3	322	11	51	57	6	780	3	63	26	29
LPF21.v1	-	-	60	69	9	665	3	25	27	27
LPF21.v2	182	6	60	70	10	715	3	30	28	30
HCF15.v1	-	-	-	69	-	-	-	-	28	29
HCF15.v2	176	6	-	69	-	-	-	-	26	29

Patients with early- (<5 years since diagnosis) or late-stage (≥5 years since diagnosis) sporadic Parkinson's disease (PD) and the one healthy control (HC) who provided multiple sampling at different visit time points: Early PD male (EPM) (with progression to late (L) disease status), late PD male (LPM), late PD female (LPF), and HC female (HCF). Time at sampling from baseline/visit (v)1 is shown in days and months. Age-at-onset, age-at-visit/sampling time, and disease duration are shown in years. Clinical information, if available for sampling days, are shown for: L-dopa equivalent daily dose (LEDD), Unified Parkinson's Disease Rating Scale three (UPDRS III), Hoehn and Yahr (H&Y score), the Montreal Cognitive Assessment (MoCA) score, and the Mini-Mental State Examination (MMSE).

Supplementary Table 2: Comorbidities and non-dopaminergic treatment related to inflammation and cognition

	HC	**PD**	**P**
Individuals with autoimmune diagnoses	**1**	**3**	ns
- Rheumatoid arthritis	1	2¤	
- Psoriasis	0	2¤	
Related anti-inflammatory treatment	**0**	**1:** Leflunomid, Prednisolon	
Individuals receiving anti-inflammatory (AI) **treatment without diagnosis: total**	**2**	**9**	ns
- Antihistamine	1	0	
- NSAID (Ibuprofen)	1	4	
- NSAID (Diclofenac)	0	2	
- Corticosteroid (Astonin)	0	1	
- Anti-microbe (Aciclovir, Quensyl)	0	2	
Total anti-inflammatory treatment	**2**	**10**	ns
Diabetic treatment (DT) (Glimepirid, Metformin, Siofor, Novorapid, rotaphane)	0	3 (only) 3 (+ND) 1 (+AI) **7 total**	ns
AI + DT	**2**	**17**	ns
Neurological drugs other than dopaminergic treatment (ND) (Amitriptylin, Cipramil, Citalopram, Clozapin, Cymbalta, Elontril, Exelon, Gabapentin, Laif, Lithium, Mirtazapin, Orfiril, Quetiapin, Remergil, Rivastigmin, Rivotril, Seroquel, Sertralin, Stangyl, Trimipramin, Valproat, Venlafaxin)	0	21 (only) 3 (+DI) 5 (+AI) **29 total**	**0.0001**
Hormone related treatment	**1**	**1**	ns
- Evista (selective estrogen receptor modulator)	1	0	
- Estragest	0	1	
Treated for any of the above (overlap)**:**	**5** (2)	**48** (9)	**0.0001**
No relevant treatment or diagnosis	**24**/29	**30**/80	**0.0001**

¤ overlap in one patient. The tow-tailed P values are shown for Fisher's exact test. Nonsteroidal anti-inflammatory drug (NSAID).

Supplementary Table 3: Fluorochromes and antibodies used for flow staining

Panel	Antigen	Fluorophore	Isotype	Clone	Host	µL/ 100	Company
Cohort#1	CD163	PE	IgG1	MAC2-158	Mouse	1	IQProducts
Cohort#1	TLR4	PerCP	IgG2a	610015	Mouse	10	Novus, R&D systems
Cohort#1	CD192 (CCR2)	FITC	IgG2a κ	K036C2	Mouse	5	Biolegend
Cohort#1	CD11b	Super Bright 780	IgG1	ICRF44	Mouse	1.25	eBioscienceTM Thermo Fischer Scientific
Cohort#1 / DC	CD14	BV421	IgG2b	Mϕp9	Mouse	3	BD Horizon
Cohort#1 /DC	CD16	PC7	IgG1	3G8	Mouse	2.5	Beckman Coulter
Cohort#1 /DC	TLR2 (CD282)	APC	recombinant	REA109		2	MACS Miltenyi Biotec
Cohort#1 /DC	HLA-DR	BV650	IgG2a κ	L243	Mouse	2.5	Biolegend
Cohort#1 /DC	CD56	ECD	IgG1	N901	Mouse	2	Beckman Coulter
Cohort#1 /DC	LIVE/DEAD™ Fixable Near-IR Dead Cell Stain Kit	633/ 635nm				0.1	Invitrogen, Thermo Fisher Scientific
DC-panel	CD141	BV510	BALB/c IgG1,K	1A4	Mouse	5	BD Horizon TM, BD
DC-panel	CD303a (BDCA-2)	PerCP-eFlour 710	IgG2a κ	201A	Mouse	5	Invitrogen
DC-panel	CD1c	PE	IgG κ	L161	Mouse	5	eBioscience TM Invitrogen
DC-panel	CD11c	FITC	IgG1 κ	B-ly6	Mouse	2	BD Pharming TM

Supplementary Table 4: Regression models to test for correlation covariance

model	dependent variant	Term	Estimate	Std Error	t Ratio	Prob >|t|	Lower 95%	Upper 95%
Simple linear regression	MoCA	disease duration	-0.017	0.090	-0.18	0.8555	-0.197	0.164
Simple linear regression	MoCA	age at visit	-0.165	0.042	-3.97	**0.0002**	-0.248	-0.082
Simple linear regression	MoCA	% live cells	-0.496	0.153	-3.23	**0.0018**	-0.802	-0.191
Simple linear regression	MoCA late only	$CD11b^-/CCR2^{dim}$	0.144	0.065	2.21	**0.0333**	0.0120	0.277
Simple linear regression	MoCA late only	% $CCR2^+$	-0.183	0.081	-2.24	**0.0311**	-0.035	-0.0175
Simple linear regression	MoCA for females	MFI CCR2 iMos	-0.004	0.001	-2.98	**0.005**	-0.007	-0.001
Multiple linear regression	MoCA	% live cells	-0.381	0.148	-2.58	**0.0117**	-0.675	-0.088
		age at visit	-0.141	0.041	-3.41	**0.001**	-0.222	-0.059
Multiple linear regression	MoCA late only	$CD11b^-/CCR2^{dim}$	0.107	0.056	1.92	0.063	-0.006	0.221
		age at visit	-0.190	0.047	-4.01	**0.0003**	-0.286	-0.094
Multiple linear regression	MoCA late only	% $CCR2^+$	-0.115	0.072	-1.58	0.1225	-0.262	0.032
		age at visit	-0.185	0.050	-3.73	**0.0006**	-0.286	-0.085
Multiple linear regression	MoCA for females	MFI CCR2 iMos	-0.003	0.001	-2.15	**0.0384**	-0.005	-0.0002
		age at visit	-0.212	0.065	-3.26	**0.0024**	-0.343	-0.080

MoCA score had in all PwP a significant correlation and simple linear regression with the percentage of live cells; and for late PD also with the fraction of $CD11b^-/CCR2^{dim}$ cells and $CCR2^+$ MNPs; and for females with PD also with the MFI of CCR2 on intermediate monocytes (iMos). MoCA was connected to age at visit, but not to disease duration. MoCA associations with the frequency of live cells and MFI of CCR2 iMos remained significant after adjusting for age, whereas the fraction of $CD11b^-/CCR2^{dim}$ and $CCR2^+$ cells did not pass the significance threshold after the covariance test, although it was a trend (0.063) for $CD11b^-/CCR2^{dim}$.

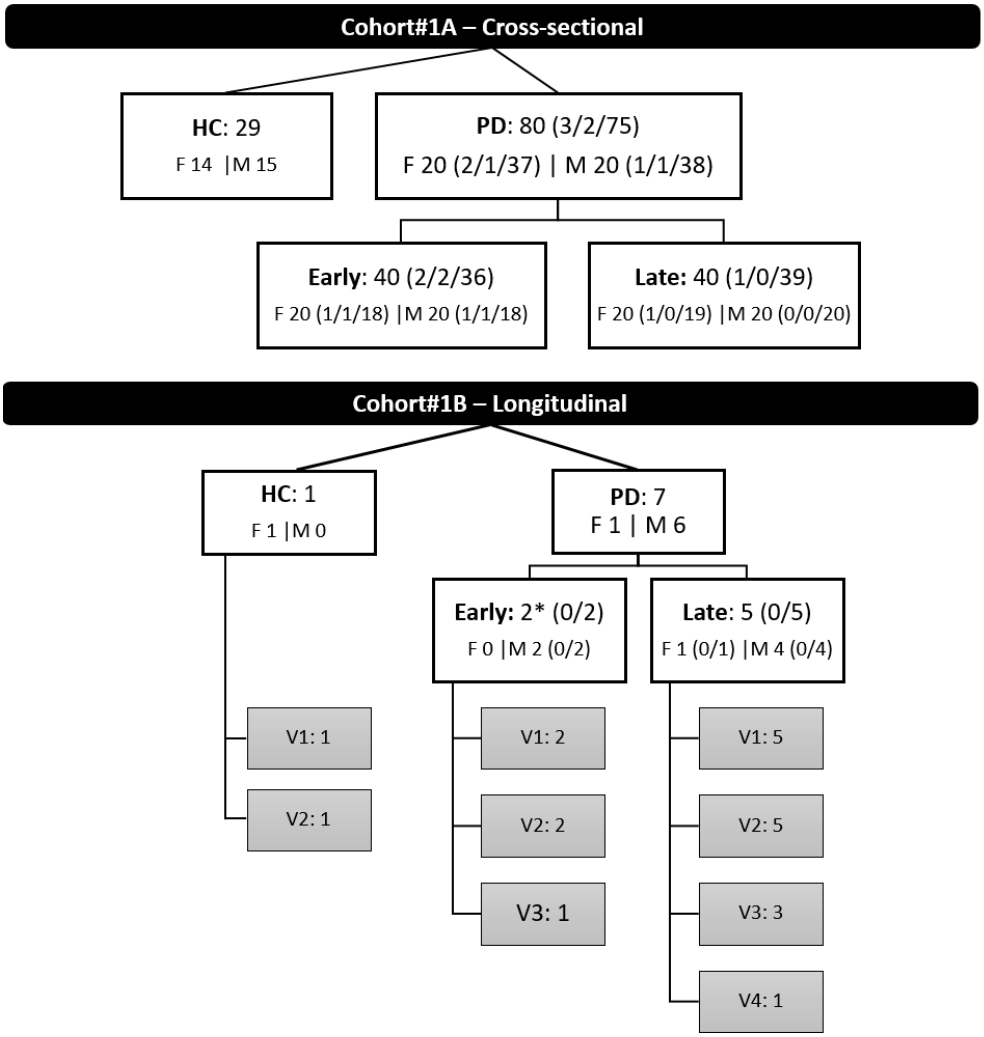

Supplementary Figure 1: Overview of study participants

The study includes samples from healthy control (HC) individuals and people with sporadic Parkinson's disease (PD) from the Hertie Biobank for Parkinson's disease at the University Hospital of Tuebingen, Germany. The cohort was subdivided into a cross-sectional Cohort#1A with 29 HC individuals and 80 people with PD, and Cohort#1B for case studies of longitudinal samples with various visit (v) numbers. Distribution of females (F) and males (M) are shown with treatments status in brackets: (unknown/untreated/treated).

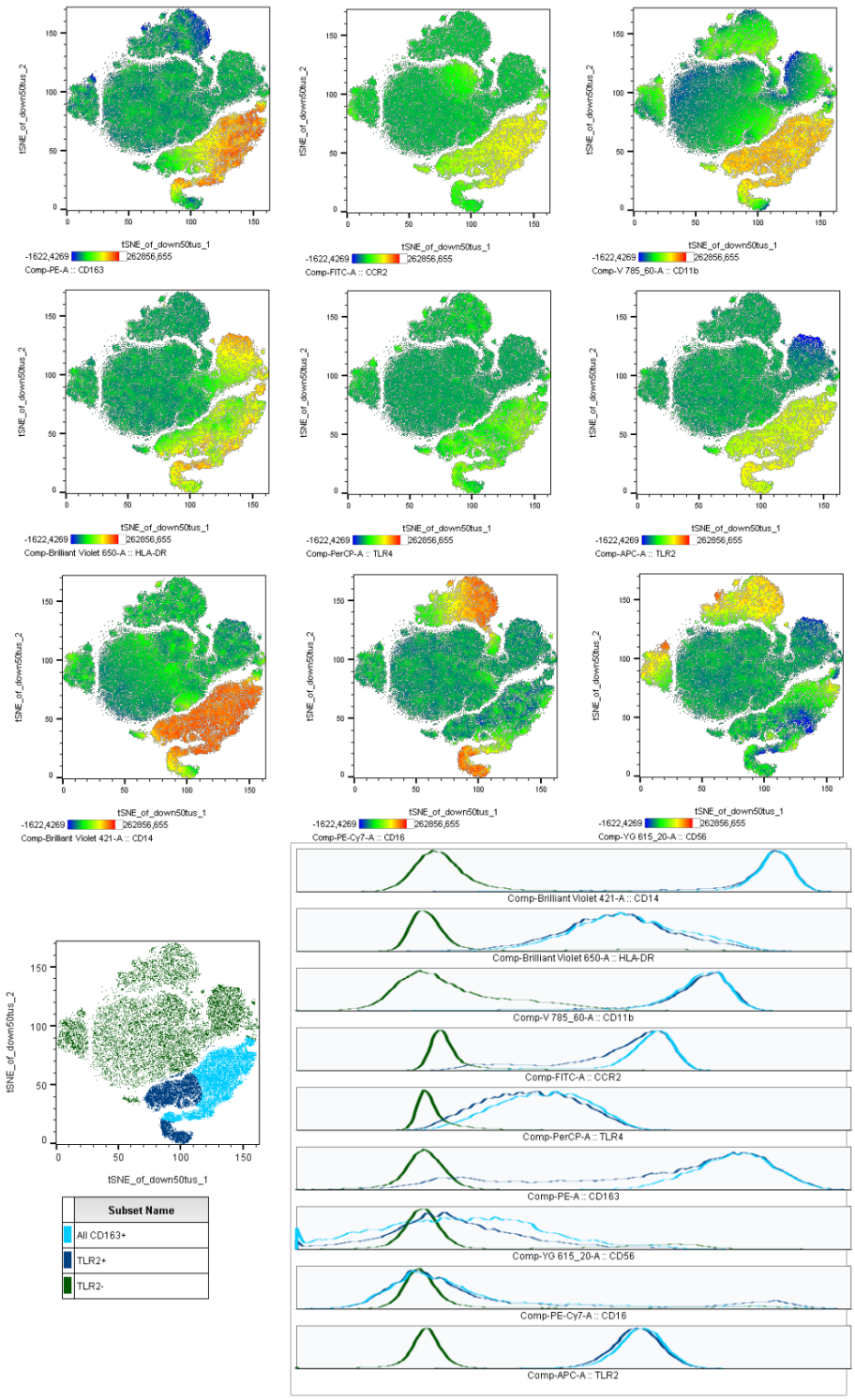

Supplementary Figure 2. Unraveling TLR2 as a mononuclear phagocyte marker
t-distributed stochastic neighbor embedding (tSNE) dimensionality reduction plots of ten concatenated samples of live cells from all PD and control groups with expression heat maps of all surface markers; and a dot plot with overlay of all TLR2^{+} cells (dark blue), all CD163^{+} cells (light blue), and TLR2^{-} cells (green); accompanied by histograms of surface makers' expression.

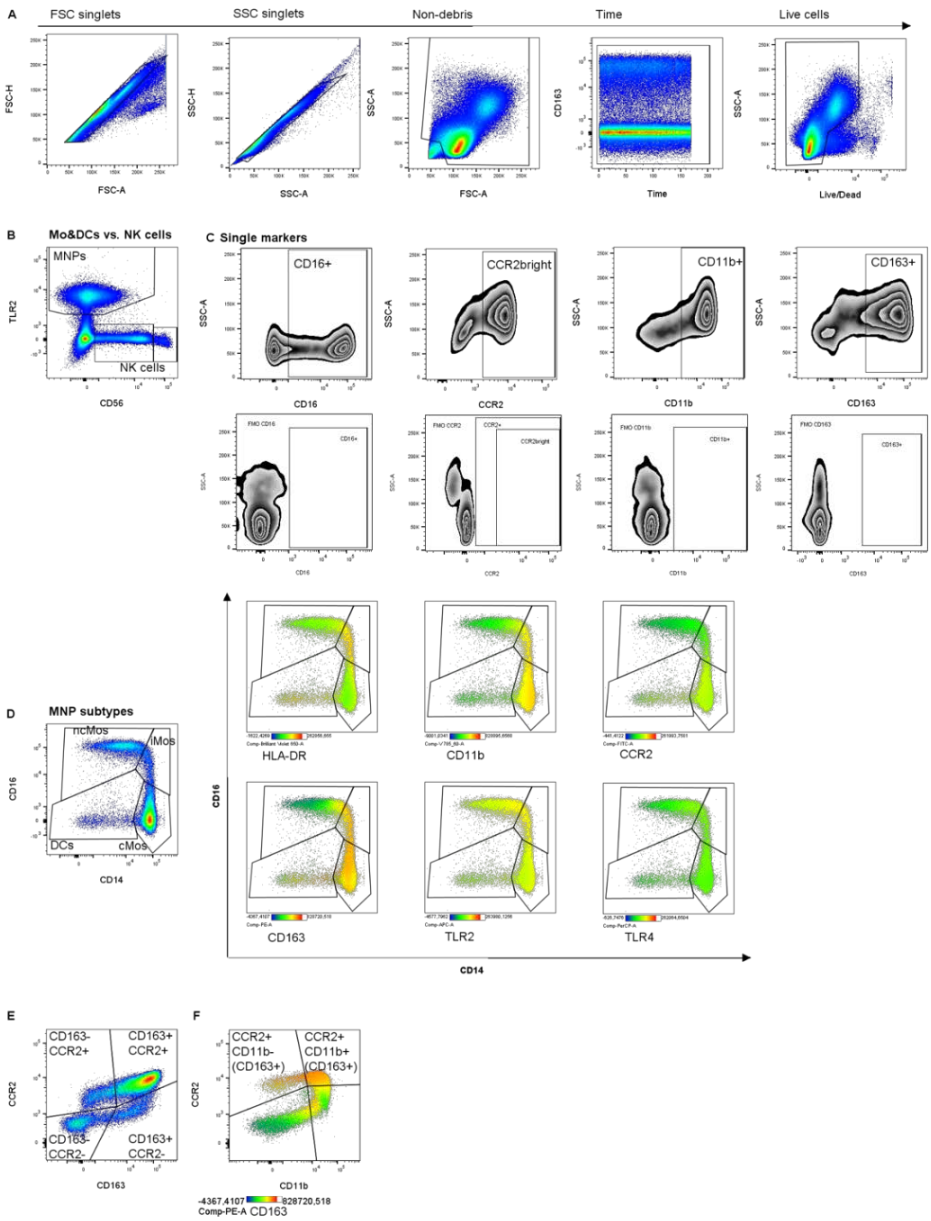

Supplementary Figure 3: Gating strategy for Cohort#1A&B

Identification of **A)** single live cells in the PBMC population base on forward scatter (FSC) and side scatter (SSC) height (H) vs. area (A), exclusion of debris, cytometer performance validation over time, followed by dead cell exclusion. **B)** Mononuclear phagocytes (MNPs) including monocytes (Mos) and dendritic cells (DCs) were identified from the live cell populations as $TLR2^{+}$; and mature and precursor natural killer (NK) cells were gated as $TLR2^{-}$ /$CD56^{dim}$ and $TLR2^{-}$/$CD56^{bright}$, respectively. **C)** Frequencies of single markers were identified using fixed gates against SSC-A for CD16 (mature NK cells only), CCR2, CD11b, and CD163 when appropriate (upper panel: full stained; lower panel: FMO controls). **D)** From the MNP gate, classical (cMos), intermediate (iMos), non-classical monocytes (ncMos), and DCs were identified based on CD14 and CD16 expression with gates adjusted based on HLA-DR heat-mapping. Heat maps are shown for other markers to visualize the MFI on the different subtypes. **E)** From the MNP gate, CD163 vs. CCR2 was gated with fixed gates, and **F)** CD11b vs. CCR2 expression was gated with adjustments made based on CD163 heat-mapping. Median fluorescence intensity (MFI) was measured on single populations; e.g. a smear for TLR4 or CCR2 (which was bright for all classical monocyte, thus no gating needed); or the positive gate only e.g. CD16.

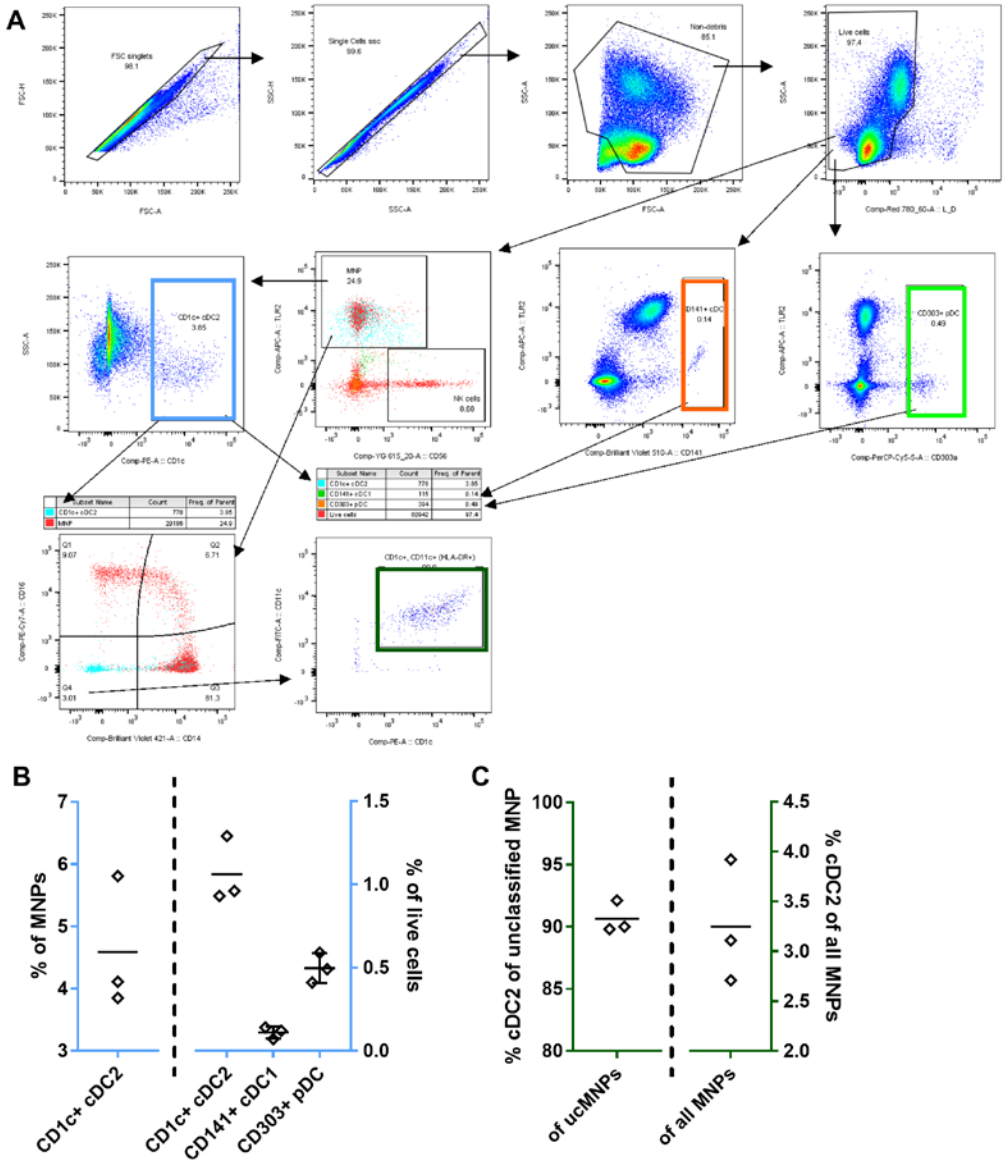

Supplementary Figure 4: Identification of dendritic cell subtypes

A control staining for dendritic cells (DCs) was performed on three control donors.
A) Similar gating approach as described in **Supp.Fig2** was used to reach MNP subtyping (Q1-4) on CD14 vs. CD16; except no gate on time. From the live cell gate, conventional (c)DC type 1 (cDC1) and plasmacytoid (p)DCs were identified as TLR2^{-}/CD141^{+} and TLR2^{-}/CD303^{+}, respectively. With a fraction of B cells (TLR2^{-}) also being CD1c^{+}, the cDC type 2 (cDC2) was identified from the MNP gate on a CD1c vs. SSC dot plot. cDC2 was back gated on to MNP subtypes (Q1-4) and to the MNP main gate together with cDC1 and pDC back-gating. From the Q4 gate on the CD14 vs. CD16 MNP subtyping dot plot, CD1c vs. CD11c was used to define the actual cDC2s within this gate. **B)** DC subtypes as percentages of MNPs or all live cells. **C)** CD1c^{+}/CD11c^{+} cDC2 percentage of the Q4 gate (termed DCs in Cohort#1) and of all MNPs.

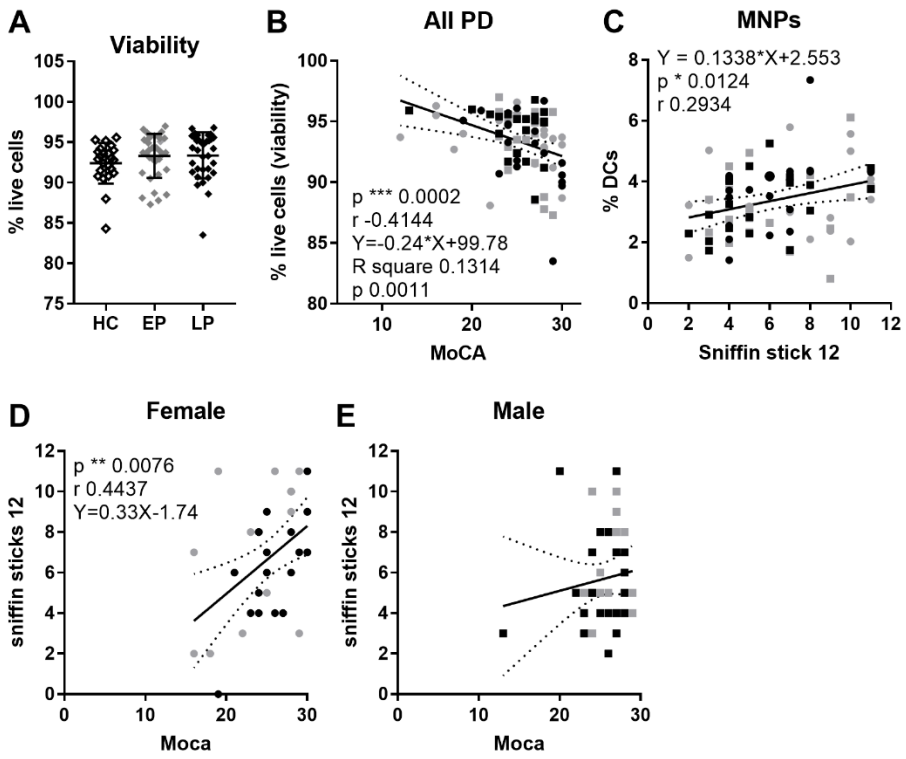

Supplementary Figure 5: Fewer dendritic cells (DCs) weakly associates with hyposmia

A) Frequency of live cells measured in the healthy control (HC), early PD (EP, <5 years since diagnosis) or late PD (LP, ≥5 years since diagnosis) groups, respectively. **B)** Variation in cell viability from PwP (symbols: female round, male square, early gray, late black) correlated negatively with the Montreal Cognitive Assessment (MoCA) scores; Spearman p and r, and linear regression equation with R square and p values are shown. **C)** Pearson correlation and linear regression of the olfaction score Sniffin' Stick 12 versus the percentage of $CD14^{-/low}/CD16^{-}$ DCs (type cDC2) within the mononuclear phagocytes (MNPs). Two outliers were removed by ROUT Q=0.01%. The linear relation was not affected by age at visit or onset, by disease duration, nor by LEDD (not shown). A correlation between MoCA and Sniffin' stick 12 olfaction scores were significant in **D)** females, but not in **E)** males; tested by Spearman correlation.

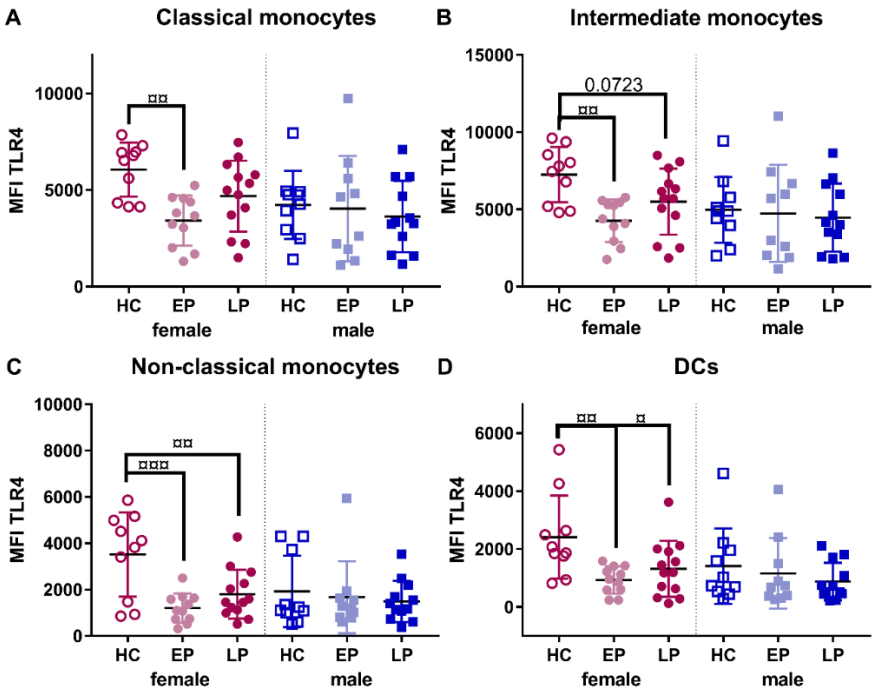

Supplementary Figure 6: TLR4 expression on monocyte subtypes and dendritic cells (DCs) is sex-dependent and decreased in PD females

Median fluorescence intensity (MFI) of TLR4 measured on the different monocyte subtypes: **A)** classical, **B)** intermediate, **C)** non-classical, and **D)** DCs in healthy control (HC), early PD (EP), and late PD (LP) groups; with early and late disease cutoff at 5 years (included in late). Female and males are separated due to priory identification of sex-differences related to TLR4 expression using t-test, with a higher level in female HCs compared to males. Statistical approach to compare same-sex samples: parametric one-way ANOVA with Tukey's multiple comparisons (¤ $p < 0.05$, ¤¤ $p < 0.01$, ¤¤¤ $p < 0.001$). TLR4 measurements are only reported for a 66 samples due to antibody lot number variance (females: 10 HC, 11 EP, 13 LP; males; 10HC, 10 EP, and 12 LP).

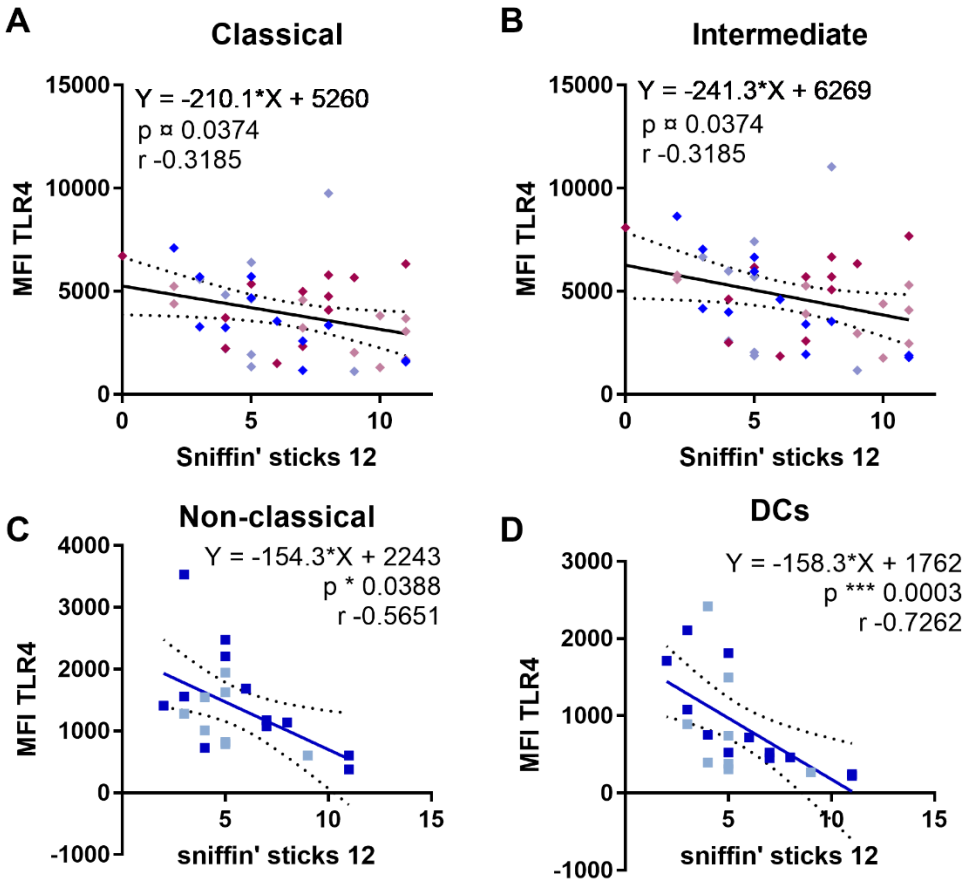

Supplementary Figure 7: Higher TLR4 expression on monocytic subtypes and dendritic cells (DCs) correlates with worse olfactory function and is sex-dependent

Median fluorescence intensity (MFI) of TLR4 measured on the different mononuclear phagocyte (MNP) subtypes: **A)** classical, **B)** intermediate, and **C)** non-classical monocytes as well as **D)** DCs in PwP for **A-B)** both sexes (cubes; male blue, female red) or **C-D)** males only (blue square). Early- (light colors) and late-stage (dark colors) PD, with cut-off at 5 years (included in late), are analyzed together and only shown as separate colors. Statistical approach: parametric Pearson (¤ $p < 0.05$) and non-parametric Spearman correlations (* $p < 0.05$, *** $p < 0.001$). TLR4 measurements are only reported on 66 samples due to AB lot number variance. Equations are shown for significant linear regressions.

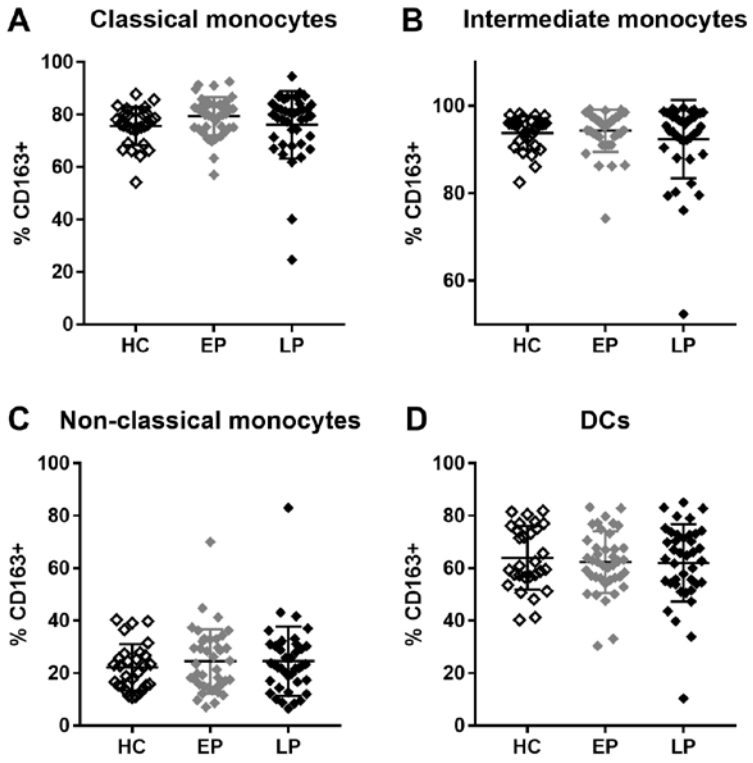

Supplementary Figure 8: Frequency of CD163^{+} cells in the different mononuclear phagocyte subtypes

Frequency of CD163^{+} cells in **A)** classical, **B)** intermediate, and **C)** non-classical monocytes, as well as **D)** dendritic cells (DCs) of the total mononuclear phagocyte (MNP) population. Healthy control (HC), early PD (EP), late PD (LP) groups.

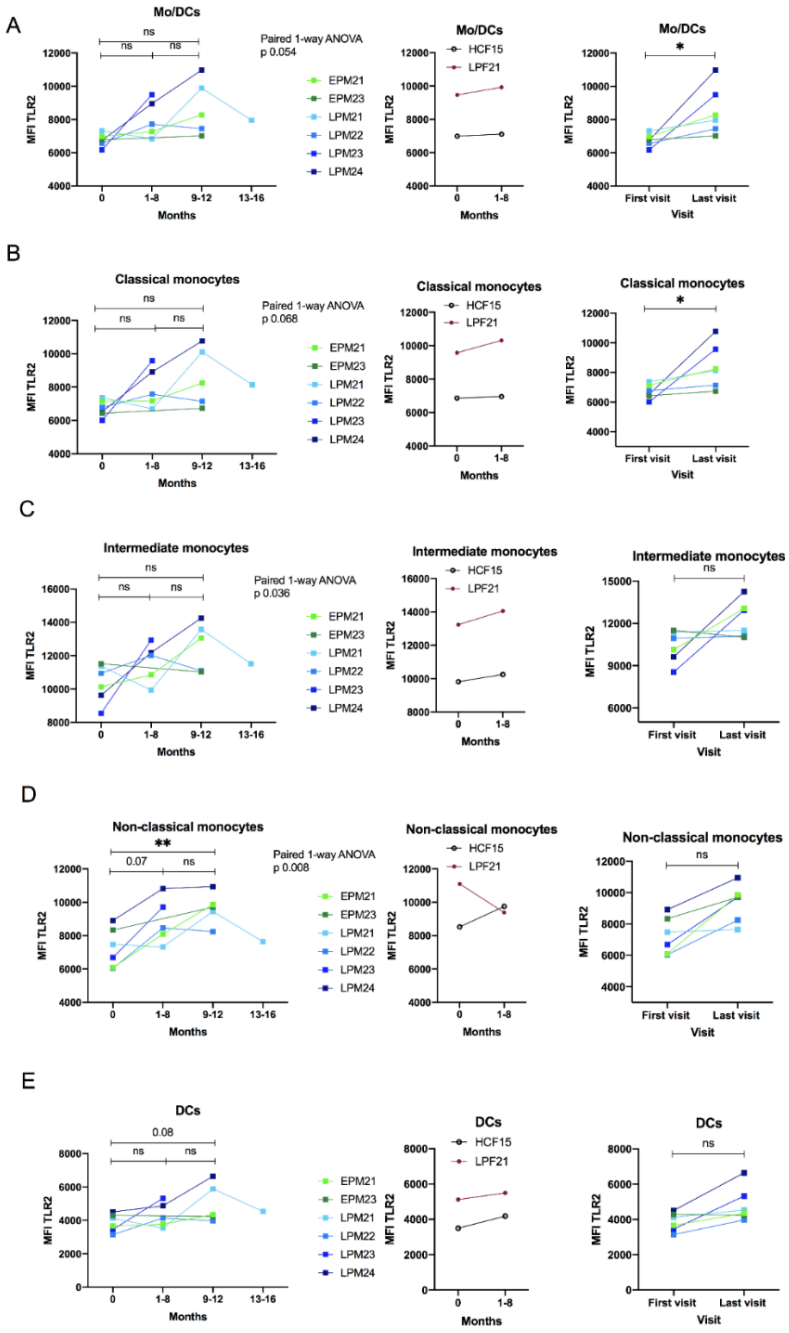

Supplementary Figure 9: Longitudinal comparison of TLR2 expression in males with PD
Median fluorescents intensity (MFI) of TLR2 on **A)** all TLR2^{+} mononuclear phagocytes (MNPs) including monocytes (Mo) and dendritic cells (DCs), and the separate subtypes: **B)** classical, **C)** intermediate, and **D)** non-classical monocytes, as well as **E)** DCs. Measured on sporadic Parkinson's disease (PD) patients with early (<5 years since diagnosis) or late (≥5 years since diagnosis) PD status and a single healthy control female (HCF) with multiple visit time points: Early PD male (EPM) (with progression to late (L)), late PD male (LPM) and female (LPF). **Left graphs:** monthly intervals of visits of all male patients: paired repeated measures mixed-effect model (REML) with Tukey's multiple comparisons; **middle graphs:** monthly intervals for LPF and HCF; **right graphs:** differences from first to last visit for all male patients: non-parametric paired t-test (Wilcoxon).* $p<0.05$, ** $p<0.01$.

References

1. Thomas GD, Hamers AAJ, Nakao C, Marcovecchio P, Taylor AM, McSkimming C, et al. Human Blood Monocyte Subsets: A New Gating Strategy Defined Using Cell Surface Markers Identified by Mass Cytometry. Arterioscler Thromb Vasc Biol. 2017;37(8):1548-58.
2. Dutertre CA, Becht E, Irac SE, Khalilnezhad A, Narang V, Khalilnezhad S, et al. Single-Cell Analysis of Human Mononuclear Phagocytes Reveals Subset-Defining Markers and Identifies Circulating Inflammatory Dendritic Cells. Immunity. 2019;51(3):573-89 e8.